Central-force model for liquid water

Howard L. Lemberg and Frank H. Stillinger

Bell Laboratories, Murray Hill, New Jersey 07974
(Received 15 October 1974)

We propose a new class of Hamiltonian models of liquid water based on resolution of the monomeric unit into three effective point charges. Interacting through central forces only, the three charges automatically assume the molecular structure. Two important effects are built into this model which have been neglected in similar attempts: intramolecular modes of vibration and the capacity for self-dissociation in the liquid phase. In addition, a large number of microsopic properties of water can be expressed in very simple terms for this representation: The pressure and internal energy, second virial coefficient, high-frequency elastic moduli, and dielectric function are discussed in explicit terms. A convenient algorithm for computing low-order quantum corrections (proportional to $\hbar^2$) to thermodynamic properties is given as well. To illustrate the general class of central-force models, we provide a concrete realization which has been determined by fitting phenomenological potentials to a nearly linear hydrogen bond of proper energy and dimer configuration. In order to elucidate the microscopic consequences of assuming central-force interactions in water, we have investigated the energy variation of small polymers (dimers and trimers) and the solvated proton near their minimum energy configurations. On a qualitative level, the results of these initial computations provide considerable encouragement for the view that water molecule interactions can be realistically approximated by linear combinations of central forces.

I. INTRODUCTION

Scientific investigators have long recognized that the physical and chemical properties of liquid water play an essential role in chemical and biological processes of great importance. It is not difficult to comprehend, therefore, the motivation that explains the great amount of effort that theoretical and experimental workers have expended in their attempts to understand the unusual and highly significant behavior displayed by H_2O.

In spite of this historical abundance of research into interactions in aqueous media, it is only recently (roughly within the last ten years) that the technological capacity has been available, in the form of large and fast computational systems, which has enabled chemists and physicists to explore the detailed consequences of several microscopic models of water subject to experimentally relevant temperatures and pressures.[1] The techniques of molecular dynamics[2] and Monte Carlo[3] computer simulation have proved invaluable aids in helping to achieve a basic understanding of the complex intermolecular interactions that occur in real water. Molecular dynamics,[4,5] in particular, has provided unique insights into the microscopic nature of equilibrium structure and transport processes in water through a detailed analysis of two specific representations of the molecular pair potential, the BNS[6] and ST2[7] models. In a number of instances these simulations have enabled the theoretician to observe phenomena that have thus far eluded experimental measurement.

In spite of successes with computer simulation, the field has not yielded easily to statistical mechanical theories more analytic in nature. By "analytic," in this context, we do not restrict attention to exactly solvable models; rather, we employ the term to describe those theoretical developments which, within a well-defined scheme of approximations, focus upon the relatively small set of properties that determine the predominant local order and short-range interactions in the liquid. Theoretical treatments of this nature provide attractive alternatives to brute force computation because of their inherently greater efficiency. But in spite of rather sophisticated attempts on several highly idealized models, the class of analytic theories remains relatively small. Among them we may cite the lattice models of Fleming and Gibbs[8] and of Bell,[9] the cell model proposed by Weres and Rice,[10] and Ben-Naim's solution of the Percus–Yevick equation for a two-dimensional fluid of "waterlike" particles.[11]

We do not believe this state of affairs to be desirable or immutable; it is, rather, a consequence of the relatively complex nature of those microscopic models that have proved useful and most realistic so far. In the spirit of attempting to overcome this barrier to theoretical progress in aqueous media, the present paper introduces a new class of phenomenological models for water. The preeminent feature of this set of models is the fact that interactions in the liquid are represented by linear combinations of central potential functions for the separate atomic species. The interaction is thus dependent explicitly only on distances, not on relative orientation, in contrast to the molecular effective potentials that have been most thoroughly investigated to date.

In order to achieve this convenient representation of the liquid-state interactions, it is necessary to displace attention from rigid molecular units to the atoms acting as effective point charges. In the limit of low densities, the set of point charges, interacting through Coulombic and non-Coulombic central forces, can be made to reproduce faithfully a number of fundamental physical properties of the basic monomeric unit. The isolated molecular geometry, dipole moment, and vibrational frequencies are among those properties that can be readily fitted for an interacting triplet of two hydrogen charges and one oxygen charge. The central-force model should thereby provide a simple representation of the effective intra- and intermolecular potential energy over a wide range of densities, from zero to the liquid density.

In addition to the intrinsic simplicity which a central-

force representation possesses, the division of the monomer into a minimal number of effective point charges enables one to take account of three additional effects which have remained thus far untreated in existing Hamiltonian models.

1. Each molecule in the liquid phase retains three intramolecular degrees of freedom, vibrating about a temperature and density-dependent internal equilibrium configuration that should be close to the equilibrium of the isolated molecule.

2. The molecular units in water undergo a small, but not insignificant, degree of dissociation into ionic components (H^+ and OH^-) which are subsequently hydrated by other H_2O molecules.

3. Quantum corrections to the semiclassical limiting expressions for statistical thermodynamic quantities may be nontrivial, owing in part to the light mass of the hydrogen atom in water.

All of these effects should be included in some manner in a quantitatively significant approach to the theory of water. While conventional wisdom holds that intramolecular vibrations can be neglected for most temperatures of interest, since $\hbar\omega_i \gg kT$ (where ω_i is the angular frequency of the ith normal mode of vibration), the influence of zero-point motions and the possibility of static distortions must still be reckoned with. The effect of molecular nonrigidity should certainly prove important in regions of high temperature or pressure. But even under more moderate conditions it should assert itself, through the nature and magnitude of the hydrogen bond distortions that occur in the liquid from the nearly ideal tetrahedral networks of ices I_c and I_h.

With respect to dissociation, one expects the influence on equilibrium structure to be relatively small, as only one molecule in 10^7 dissociates under ordinary circumstances. However, the ability of the molecules to dissociate must certainly play an essential role in important nonequilibrium processes such as electrical conduction. Furthermore, the dissociation process in pure water becomes enormously enhanced at elevated temperature and pressure. Finally, we point out that fundamental understanding of pH and the kinetics of rapid chemical reactions involving proton transfer—for which quantum effects must certainly be important—can best be understood on the basis of a definite model such as that advocated here.

In Sec. II we describe in a systematic fashion the criteria to be satisfied by a set of phenomenological central potentials for water, and display a specific triad of functions—not necessarily the optimum set—which has been fitted to a small number of characteristics of the monomer and dimer. For the sake of completeness we include Sec. III, which comprises a theoretical framework relating chemical and physical properties of "central-force water" to a multicomponent formulation of the statistical mechanics of simple fluids. Because of the seemingly drastic approximations entailed in limiting water molecule interactions in the way we have, the minimum-energy structures and energy variation of water dimers, trimers, and solvated ions have been considered. These excursions in the appropriate configuration spaces are analyzed in Secs. IV–VI. Finally, the conclusions and speculations which emerge from the present study, as well as prospects for future investigation, are summarized in Sec. VII.

II. DESCRIPTION OF THE MODEL

Since the proposal of a three-charge model by Bernal and Fowler[12] some forty years ago, the representation of water molecule interactions by point-charge attractions and repulsions has provided one of the most enduring and flexible frameworks for theoretical treatment of water. Among the other point-charge models which have figured prominently in the development of a statistical mechanical theory of water, we may mention those of Verwey,[13] Rowlinson,[14] and Bjerrum[15]; there have been a host of other papers as well. Most of these theoretical efforts represented attempts to extend agreement with experimentally observed quantities beyond those touched upon by Bernal and Fowler. In the process, new complications were introduced, either by shifting the positions of the original point charges or by inserting additional ones. The latter course of development is exemplified by a recent paper of Shipman and Scheraga,[16] proposing a resolution of the molecule into seven point charges, with the intent of formulating an accurate empirical intermolecular potential.

While we acknowledge the value of a quantitatively accurate potential function, the practical utility of a model with a large number of interacting centers in each molecule is severely limited from the standpoint of statistical mechanical computations. Even the tetrahedral four-charge BNS formulation,[6] similar in spirit to the Bjerrum treatment, has been thoroughly investigated only by time-consuming calculations.[4,10]

Our objective in this paper is to recapture the simplicity that is necessary for reasonably detailed calculations on a point-charge molecular model of water. Thus we propose a three-charge microscopic picture of water somewhat similar to the one suggested by Bernal and Fowler. We postulate a general class of potential functions to describe the point-charge–point-charge interactions, encompassing Coulombic and non-Coulombic contributions, and discuss the specific constraints that should be imposed upon these potential functions to produce the proper intramolecular and intermolecular bonding. As an illustration, a concrete realization of the set of potential functions is provided which has been determined by a fit to structural and dynamical properties of the monomer and dimer.

In order to ensure that our model incorporates intramolecular degrees of freedom and a capacity for dissociation, yet remain conceptually and computationally simple, we require that the centers of mass concentration and the centers of charge concentration in the water molecule coincide. The natural resolution of the molecule into point charges satisfying this criterion is as follows: Each molecule is comprised of two effective charges $+q$ located at the equilibrium positions of the H's, and one effective charge $-2q$ located at the equilibrium position of the O. The arrangement of charges in the monomer is shown in Fig. 1.

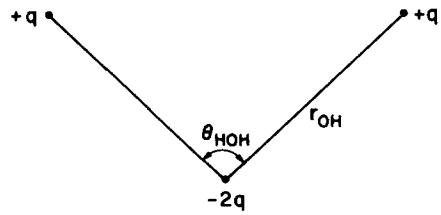

FIG. 1. Point-charge representation of the water molecule which corresponds to the central-force model. A value of $0.32983e$ for the effective charge of yields a dipole moment in agreement with experiment, for the measured parameters $r_{OH} = 0.9584$ Å, $\theta_{HOH} = 104.45°$.

The ratio of charges on the "hydrogen ions" and "oxygen ions" assures electroneutrality of individual H_2O molecules. Since the assignment of effective charges is intended to represent the dominant electrostatic interactions within *and* among molecules, it is logical to determine the magnitude of q by a fit to the experimentally observed dipole moment μ, which has been measured as 1.86 D.[17] Using this value and the isolated molecule structural parameters reported by Kern and Karplus,[18] $r_{OH} = 0.9584$ Å and $\theta_{HOH} = 104.45°$, we therefore find

$$q = \frac{\mu}{2r_{OH}\cos\frac{1}{2}\theta_{HOH}} = 0.32983e\,. \tag{2.1}$$

The fractional charge reflects the extent of shielding of the full protonic charge by the ten electrons in each molecule.

To produce an O–H molecular bond at small OH distances, the potential function describing oxygen–hydrogen interactions should have a deep attractive well with absolute minimum at $r_{OH} = 0.9584$ Å; for $r_{OH} < 0.9584$ Å, the potential should rise sharply to large positive values. We generate such functional behavior with a linear combination of two inverse powers, one of which represents the attractive interaction between a hydrogen ion of charge $+q$ and an oxygen ion of charge $-2q$. The remaining inverse power term must subsume the necessary repulsive interactions; it is characterized by an exponent $n \gg 1$ that remains to be determined. Thus, we define a family of central potentials $v_{OH}(r)$ of general form

$$v_{OH}(r) = \frac{2q^2}{r_{OH}}\left[\frac{1}{n}\left(\frac{r_{OH}}{r}\right)^n - \frac{r_{OH}}{r}\right]. \tag{2.2}$$

Further requirements (on the equilibrium structure of small H_2O polymers, for example) may make it desirable to append additional terms to (2.1), but this form is sufficient to create molecular binding between hydrogen and oxygen "effective ions."

We proceed next to the determination of a hydrogen–hydrogen effective pair potential, $v_{HH}(r)$. Once again we expect a Coulombic contribution, in this case, repulsive. A short-range repulsive interaction which grows more rapidly than $1/r^2$ is expected as well. Because H_2O is a nonlinear triatomic molecule, these cannot be the only contributions. Indeed, in order to reproduce this geometry with central-force interactions alone, $v_{HH}(r)$ must have a local minimum at the single-molecule HH distance of $r_{HH} = 1.5151$ Å. A general form for $v_{HH}(r)$ may thus be written as

$$v_{HH}(r) = q^2/r + f(r)\,, \tag{2.3}$$

the undetermined function $f(r)$ including the appropriate attractions and repulsions described above. One further physical requirement on $v_{HH}(r)$ is that linearization of the molecule (i.e., opening of θ_{HOH} to 180°) be thermally unfavorable. At the stable OH separation, this amounts to the constraint

$$v_{HH}(1.5151\text{ Å}) < v_{HH}(1.9168\text{ Å})\,. \tag{2.4}$$

The unknown exponent n of (2.2), as well as the curvature of the function $f(r)$ at 1.5151 Å, are determined by requiring that the point-charge water molecule of Fig. 1 have normal modes of vibration in accord with those experimentally observed.[19] In general, the nonlinear triatomic H_2O has four harmonic force constants on account of its C_{2v} symmetry, but within the central-force approximation, only two of these are independent. The asymmetric stretch depends only on the OH curvature at its minimum, so we fix n by fitting to it[20]:

$$v''_{OH}(r_{OH}) = 7.9699\times10^5\text{ dyn/cm}\,,\qquad n = 14.9797\,. \tag{2.5}$$

As a result, we have

$$v_{OH}(r) = \frac{2.66366}{r^{14.9797}} - \frac{72.269}{r}\,, \tag{2.6}$$

with distance measured in Å and energy in kcal/mole.

The two symmetric modes of vibration cannot be fitted simultaneously with the single remaining force constant, $v''_{HH}(r_{HH})$. However, we can equalize the discrepancies in the resulting normal mode frequencies (at 14.4%) by choosing $v''_{HH}(r_{HH}) = 1.7865\times10^5$ dyn/cm.[20] This in turn implies that $f''(r_{HH}) = 1.6421\times10^5$ dyn/cm. One combination of simple functions which has been found to satisfy all of the above requirements on $v_{HH}(r)$ is

$$v_{HH}(r) = \frac{36.1345}{r} + \frac{30.}{1+\exp[21.9722(r-2.125)]} - 26.51983\exp[-4.728281(r-1.4511)^2]\,. \tag{2.7}$$

The two potential functions (2.6) and (2.7) are employed throughout this paper in our assessment of the feasibility of a central-force model for water.

Having determined $v_{HH}(r)$ and $v_{OH}(r)$, we must now specify a third potential, $v_{OO}(r)$, in order to completely establish the model. This third function should give rise to purely repulsive forces between two oxygen ions, for it must prevent the formation of an OH bond of molecular strength between a hydrogen on one molecule and the oxygen ion of a nearest neighbor. On the other hand, the forces entailed by $v_{OO}(r)$ should promote hydrogen bonding between neighboring molecules of the proper strength and range.

One contribution to the oxygen–oxygen interactions will be the normal repulsion of two similarly charged ions. The remaining portion we determine by fitting the interaction energy of two rigid molecules in a hydrogen-bonded configuration to a representative energy, -6.5 kcal/mole. The configuration selected for this procedure was the optimal hydrogen bond of the recent ST2 model

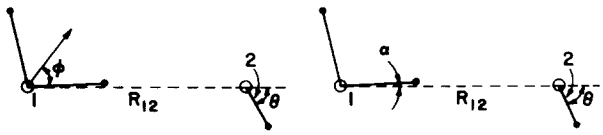

ST2-SE DIMER CF-SE DIMER

(a) (b)

FIG. 2. (a) Most stable dimer of the ST2 potential, a symmetric eclipsed configuration, with $R_{12}=2.852$ Å, $\theta=51.8°$, $\varphi=53.6°$. (b) Most stable dimer for central force potentials (2.6)–(2.8), allowing for unconstrained bond lengths and angles. The optimized parameter values for this symmetric eclipsed arrangement are $R_{12}=2.865$ Å, $\theta=60.7°$, $\alpha=0.96°$. Bond angles are $\theta=102.2°$, $\theta_2=105.0°$; bond lengths (from left to right) are 0.9602 Å, 0.9714 Å, 0.9602 Å, 0.9602 Å.

[depicted in Fig. 2(a)], with an OO separation of 2.85 Å and donor and acceptor angles of 51.8° and 53.6°, respectively. A Lennard-Jones combination of inverse powers was employed as the specific functional form for the non-Coulombic part of $v_{OO}(r)$, with the final result

$$v_{OO}(r)=\frac{144.538}{r}+\frac{1.69712\times10^6}{r^{12}}-\frac{4.03939\times10^3}{r^6}. \tag{2.8}$$

The set of functions (2.6)–(2.8) is one of an infinity of such sets which satisfy the criteria outlined above. In addition, the molecules are stable with respect to the disproportionation reaction

$$2H_2O \rightarrow H_3O^+ + OH^-, \tag{2.9}$$

which is energetically unfavorable by $v_{HH}(1.5151\text{ Å})$ per mole of H_3O^+. The variation of the central potentials (2.5)–(2.7) with distance is illustrated in Fig. 3. Although we anticipate later revisions, we believe that this set is sufficiently representative of true water molecule interactions to proceed with further analysis.

III. GENERAL PROPERTIES OF THE CENTRAL-FORCE MODEL

A. Pressure and internal energy

It is appropriate to begin a theoretical discussion by defining ion–ion pair correlation functions for the model. In a system of N oxygen and $2N$ hydrogen ions, the potential energy $V_{N,2N}$ is a superposition of the three pairwise-additive central potentials v_{OH}, v_{HH}, and v_{OO}:

$$V_{N,2N}=V_{N,2N}(\{\mathbf{r}\})=\frac{1}{2}\sum_{\substack{j,k=1\\ j\neq k}}^{3N} v_{jk}(r_{jk}). \tag{3.1}$$

Here, and throughout this paper, we assume particles $1, 2, \ldots, N$ are oxygens, while $N+1, N+2, \ldots, 3N$ are hydrogens.

The pair correlation functions in a canonical ensemble can be defined by ($\rho=N/V$, $\beta=1/k_BT$)

$$g_{OO}(r_{12})=\frac{N(N-1)}{\rho^2}\,\frac{\int d\mathbf{r}_3\cdots d\mathbf{r}_{3N}\exp(-\beta V_{N,2N})}{Z_{N,2N}}, \tag{3.2a}$$

$$g_{OH}(r_{1,N+1})=\frac{2N\cdot N}{2\rho\cdot\rho}\times\frac{\int d\mathbf{r}_2\cdots d\mathbf{r}_N d\mathbf{r}_{N+2}\cdots d\mathbf{r}_{3N}\exp(-\beta V_{N,2N})}{Z_{N,2N}}, \tag{3.2b}$$

$$g_{HH}(r_{N+1,N+2})=\frac{2N(2N-1)}{(2\rho)^2}\times\frac{\int d\mathbf{r}_1\cdots d\mathbf{r}_N d\mathbf{r}_{N+3}\cdots d\mathbf{r}_{3N}\exp(-\beta V_{N,2N})}{Z_{N,2N}}, \tag{3.2c}$$

where the configurational partition function $Z_{N,2N}$ is just

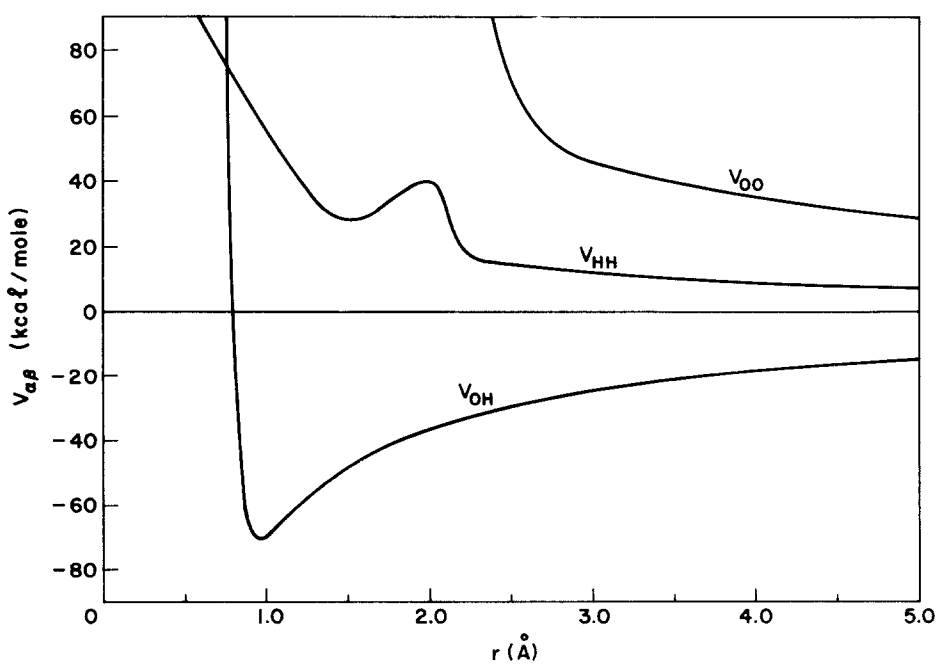

FIG. 3. Interaction potentials between effective oxygen and hydrogen ions, Eqs. (2.6)–(2.8), for the present central-force model of water.

$$Z_{N,2N} = \int d\mathbf{r}_1 \cdots d\mathbf{r}_{3N} \exp(-\beta V_{N,2N}) . \tag{3.3}$$

The pair correlation functions, as defined, are normalized to unity at large distance in the thermodynamic limit $N \to \infty$, $V \to \infty$, $\rho = N/V =$ constant. From Eq. (3.2), it is easy to show in this limit that the prevailing electroneutrality can be expressed in either of the alternative forms

$$\rho \int [g_{OH}(r) - g_{OO}(r)]\, d\mathbf{r} = 1 , \tag{3.4a}$$

or

$$2\rho \int [g_{OH}(r) - g_{HH}(r)]\, d\mathbf{r} = 1 . \tag{3.4b}$$

Somewhat more difficult to prove, but nevertheless an exact result, is the corresponding second-moment condition[21]

$$\int [2g_{OH}(r) - g_{OO}(r) - g_{HH}(r)] r^2 d\mathbf{r} = 3k_B T/8\pi\rho^2 q^2 , \tag{3.5}$$

a consequence of the collective correlations that persist at large distances in a fluid with long-range Coulomb interactions.

The pressure exerted by the system is found from the volume derivative of the Helmholtz free energy. By using Green's coordinate-scaling technique, one finds

$$\beta p = 3\rho - \tfrac{1}{6}\beta\rho^2 \left\{ \int d\mathbf{r}\, \mathbf{r} \cdot [g_{OO}(r)\nabla v_{OO}(r) + 4g_{OH}(r)\nabla v_{OH}(r) + 4g_{HH}(r)\nabla v_{HH}(r)] \right\} . \tag{3.6}$$

In the limit of low densities, it can be shown that molecular binding of HOH triplet reduces (3.6) to the expected relation $\beta p = \rho$.

In a similar manner, the system thermodynamic energy can be related to integrals over the correlation functions. We have an average potential energy

$$\langle U \rangle = \frac{1}{Z_{N,2N}} \int d\mathbf{r}_1 \cdots d\mathbf{r}_{3N} V_{N,2N}(\{\mathbf{r}\}) \exp(-\beta V_{N,2N}) = -\frac{1}{Z_{N,2N}} \frac{\partial Z_{N,2N}}{\partial \beta} . \tag{3.7}$$

Substitution of (3.1) in this expression and integration over all coordinates, save one, in each term of the sum gives the multicomponent form of a well-known formula for internal energy $\langle E \rangle$:

$$\langle E \rangle / N = \tfrac{3}{2} k_B T + \tfrac{1}{2}\rho \int d\mathbf{r} v_{OO}(r) g_{OO}(r) + 2\rho \int d\mathbf{r} v_{HH}(r) g_{HH}(r) + 2\rho \int d\mathbf{r} v_{OH}(r) g_{OH}(r) . \tag{3.8}$$

B. Virial series

Standard formulas are available for virial coefficients $B(T)$, $C(T)$, ..., for the vapor phase equation of state,[22]

$$p/\rho kT = 1 + B(T)\rho + C(T)\rho^2 + D(T)\rho^3 + \cdots , \tag{3.9}$$

in terms of integrals involving intermolecular interactions. These integrals (and the virial series itself at small ρ) converge provided the constituent molecules are uncharged. Under ordinary temperature and pressure conditions this is adequately satisfied for water, for even in the liquid only one molecule in 10^7 is dissociated. But since dissociation *is* possible in our central-force model for water, and since the model will eventually be applied under extreme temperature and pressure conditions where dissociation becomes frequent, special consideration should be given to the virial expansion.

Because the central-force model treats water as an unsymmetrical fused electrolyte, theories of electrolytes are in principal relevant. But since water is normally so weakly ionized, it is meaningful to introduce the dissociation constant K_1 for the first ionization reaction:

$$H_2O \rightleftarrows H^+ + OH^- . \tag{3.10}$$

If x represents the fraction of molecules which are dissociated,

$$K_1 = \rho x^2/(1-x) , \tag{3.11}$$

$$x \cong (K_1/\rho)^{1/2} . \tag{3.12}$$

Obviously x will be very small in the vapor, unless the temperature is very high. For completeness, we note that the infrequent ions at concentration ρx will in principle cause appearance of a Debye–Hückel term in the small-ρ pressure equation:

$$\frac{p}{k_B T} = 1 - \frac{1}{3\pi}\left(\frac{2\pi\rho x q^2}{k_B T}\right)^{3/2} + B(T)\rho^2 + \cdots , \tag{3.13}$$

where we have disregarded x in the standard second virial coefficient term. Under ordinary circumstances, the Debye–Hückel term has no numerical significance.

To agree with the failure of virtually all molecules to dissociate, suitable integration limits must be appended to the virial coefficient integrals. For the present purposes, we can simply require that the OH bond lengths not exceed an upper limit L. Any bond stretched beyond length L therefore would be considered "broken," that is, the molecule would be regarded as dissociated. A reasonable choice for L would be

$$L = 1.5 \text{ Å} , \tag{3.14}$$

considering that the equilibrium bond length is just under 1 Å, and that rms vibrational amplitudes are only about 0.05–0.10 Å.

By following the standard derivation of cluster series for the partition function, with suitable minor modifications for present application, one finds

$$B(T) = -\frac{1}{2V} \int_{(L)} \frac{d\mathbf{S}_1}{Q_1} \int_{(L)} \frac{d\mathbf{S}_2}{Q_1} \{\exp[-\beta V^{(2)}(\mathbf{S}_1, \mathbf{S}_2)] - \exp[-\beta V^{(1)}(\mathbf{S}_1) - \beta V^{(1)}(\mathbf{S}_2)]\} , \tag{3.15}$$

where

$$Q_1 = \frac{1}{V}\int_{(L)} d\mathbf{S}_1 \exp[-\beta V^{(1)}(\mathbf{S}_1)]\,. \tag{3.16}$$

The vectors $\mathbf{S}_1$ and $\mathbf{S}_2$ comprise the configurational coordinates for the respective molecules. $V^{(1)}$ stands for the three intramolecular central-force interactions and $V^{(2)}$ collects all fifteen central-force interactions for two molecules. The integration constraint denoted by (L) enforces the bond length condition advocated above.

Similar, but more complicated, expressions can be derived for higher-order virial coefficients. The specific form adopted by the third virial coefficient is

$$C(T) = -\frac{1}{3V}\int_{(L)}\frac{d\mathbf{S}_1}{Q_1}\int_{(L)}\frac{d\mathbf{S}_2}{Q_1}\int_{(L)}\frac{d\mathbf{S}_3}{Q_1}\exp[-\beta V^{(1)}(\mathbf{S}_1)-\beta V^{(1)}(\mathbf{S}_2)-\beta V^{(1)}(\mathbf{S}_3)]\,f(\mathbf{S}_1,\mathbf{S}_2)f(\mathbf{S}_1,\mathbf{S}_3)f(\mathbf{S}_2,\mathbf{S}_3)\,, \tag{3.17}$$

$$f(\mathbf{S}_i,\mathbf{S}_j) = \exp[-\beta V^{(2)}(\mathbf{S}_i,\mathbf{S}_j)+\beta V^{(1)}(\mathbf{S}_i)+\beta V^{(1)}(\mathbf{S}_j)]-1\,. \tag{3.18}$$

C. High-frequency elastic moduli

Zwanzig and Mountain[23] have provided an integrated formulation of the frequency-dependent elastic and viscous responses of a simple monatomic fluid. For the special case of central-force interactions, it is found that the high-frequency limits of the shear and bulk moduli are particularly easily expressed in terms of the pair correlation function. It is a compelling theoretical motivation for investigating central-force models of polyatomic fluids that these same high-frequency transport coefficients are readily expressed through multicomponent generalization of this simple theory.

By a mathematical analysis similar to Zwanzig and Mountain, we find

$$G_\infty = 3\rho k_B T + \frac{2\pi\rho^2}{15}\int_0^\infty dr\left\{g_{OO}(r)\frac{d}{dr}[r^4 v'_{OO}(r)]+4g_{OH}(r)\frac{d}{dr}[r^4 v'_{OH}(r)]+4g_{HH}(r)\frac{d}{dr}[r^4 v'_{HH}(r)]\right\}, \tag{3.19}$$

$$K_\infty = 2\rho k_B T + p + \frac{2\pi\rho^2}{9}\int_0^\infty dr\, r^3\left\{g_{OO}(r)\frac{d}{dr}[r v'_{OO}(r)]+4g_{OH}(r)\frac{d}{dr}[r v'_{OH}(r)]+4g_{HH}(r)\frac{d}{dr}[r v'_{HH}(r)]\right\}, \tag{3.20}$$

for the shear and bulk moduli of water, respectively. Combining these expressions with Eq. (3.8) for the virial pressure, it is seen that

$$K_\infty = \tfrac{5}{3}G_\infty + 2(p - 3k_B T) \tag{3.21}$$

is the appropriate generalization of Cauchy's identity relating the shear and bulk responses.

Some comment is in order on the meaning of the high-frequency limit just discussed. It is clear from the derivations of Zwanzig and Mountain that the frequency is to be regarded as much greater than any of the "natural frequencies" of the system of particles. For our assembly of oxygen and hydrogen ions the highest of these natural frequencies are the intramolecular modes of vibration. Thus, the high-frequency limit for central force water is elevated considerably above the frequency range where K_ω and G_ω reach plateau values for simple fluids ($\approx 10^{10}$ Hz). As a consequence, the quantities K_∞ and G_∞ defined above may not be susceptible to determination by standard ultrasonic methods.

D. Equal-time quantum corrections

We now develop leading-order quantum corrections to the canonical weighting function $\exp(-\beta E)$ for the class of central-force models described in the present paper. In this manner, a general method is obtained for evaluating quantum corrections to any thermodynamic property of water.

The quantum Hamiltonian determining the wavefunctions $\Psi_\alpha(\mathbf{r}^{3N})$ of the system of N oxygen anions and $2N$ hydrogen cations is

$$\hat{\mathcal{H}} = \sum_{j=1}^{3N}\frac{-\hbar^2}{2m_j}\nabla_j^2 + V(\mathbf{r}^{3N})\,. \tag{3.22}$$

The normalized density operator may thus be expressed as

$$\hat{\rho}_{3N} = \frac{1}{Q_{3N}(\beta)}e^{-\beta\hat{\mathcal{H}}} \tag{3.23}$$

in the canonical ensemble, with partition function

$$Q_{3N}(\beta) = \mathrm{Tr}(e^{-\beta\hat{\mathcal{H}}}) = \sum_\alpha\int d\mathbf{r}^{3N}\Psi_\alpha^*(\mathbf{r}^{3N})e^{-\beta\hat{\mathcal{H}}}\Psi_\alpha(\mathbf{r}^{3N})\,. \tag{3.24}$$

Nuclear exchange effects will be neglected, an assumption which should be valid in the temperature range of interest.

In developing a quantum expansion for the density matrix it will be assumed that the various pair potentials $v_{jk}(r_{jk})$ are sufficiently well behaved that the Wigner–Kirkwood[24] expansion can be employed. Choosing a basis set of free-particle eigenfunctions, we find the following expansion for the diagonal density matrix elements:

$$\rho_{3N}(\mathbf{r}^{3N};\mathbf{r}^{3N}) = \frac{\exp[-\beta V(\mathbf{r}^{3N})]}{Z_{3N}(\beta)}\left[1+\beta\hbar^2\left(\frac{1}{24}\sum_j\frac{1}{m_j}(\nabla_j\beta V)^2-\frac{1}{12}\sum_j\frac{1}{m_j}(\nabla_j^2\beta V)\right)\right], \tag{3.25}$$

where $Z_{3N}(\beta)$ is the configurational partition function. For the sake of consistency, it should be evaluated to $O(\hbar^2)$. Equation (3.25) may be expressed in a more enlightening way as

$$\rho_{3N}(\mathbf{r}^{3N};\ \mathbf{r}^{3N}) = \frac{\exp[-\beta W(\mathbf{r}^{3N})]}{Z_{3N}(\beta)}, \tag{3.26}$$

with

$$W(\mathbf{r}^{3N}) = V(\mathbf{r}^{3N}) + \hbar^2 \sum_j \frac{1}{m_j}\left[\tfrac{1}{12}\nabla_j^2 \beta V - \tfrac{1}{24}(\nabla_j \beta V)^2\right], \tag{3.27}$$

and

$$Z_{3N}(\beta) = \int d\mathbf{r}^{3N} \exp[-\beta W(\mathbf{r}^{3N})]. \tag{3.28}$$

Even if $V(\mathbf{r}^{3N})$ is pairwise additive, the quantum-corrected potential contains effective three-body interactions because of the presence of the gradient-squared terms. This fact makes the evaluation of quantum corrections to static properties in general a nontrivial task. For calculating low-order corrections to thermodynamic properties, however, one may use integration by parts to simplify (3.28) considerably. In this case, if $V(\mathbf{r}^{3N})$ is equivalent to a sum of central potential functions, then so is $W(\mathbf{r}^{3N})$, with component potentials

$$w_{\alpha\beta}(r) = v_{\alpha\beta}(r) + \frac{\beta\hbar^2}{24 m_{\alpha\beta}} \nabla^2 v_{\alpha\beta}(r), \tag{3.29}$$

when used to calculate the Helmholtz free energy. The parameter $m_{\alpha\beta}$ is a reduced mass for the $\alpha\beta$ pair.

Thus, to second-order in $\hbar$, thermodynamic quantum effects may be understood in classical terms with a temperature-dependent "apparent potential" W that depends not only on the true classical energy, but also on its curvature. The additional term has the following physically relevant effect on the shape of the quantum "apparent potential."

Regions of positive curvature (as in the vicinity of minima) are raised, while regions of negative curvature (such as maxima) are lowered, producing diminished variation. The net effect of this modification at a given temperature is that the potential energy will be less effective in localizing particles relative to one another. Consequently the peaks of the pair correlation functions should be somewhat broader than if $V(\mathbf{r}^{3N})$ alone were used.

In contrast to the simple prescription explained above, the evaluation of terms of the Wigner–Kirkwood series for molecular models with noncentral interactions is an extremely complex problem. For models based on rigid monomeric units the issue is one of generating quantum corrections for the asymmetric top; this question has not yet been quantitatively resolved.

E. Dielectric response

A convenient expression for the wavelength and frequency-dependent dielectric constant $\epsilon(k, \omega)$ of "central-force water" may be derived by considering the effect that an applied electric potential

$$\Phi_{ap}(\mathbf{r},\ t) = \Phi_0 \exp[i(\mathbf{k}\cdot\mathbf{r} + \omega t)] \tag{3.30}$$

has on an assembly of N oxygen and $2N$ hydrogen ions. Since the dielectric constant measures the linear response of the system, the potential (3.30) should be turned on adiabatically, starting at some point in the distant past. In order to accomplish this we imagine ω to have a small negative imaginary part, $\omega = \omega_r - i\epsilon$, and take the limit $\epsilon \to 0$ at the end of the calculation.

The applied field arising from (3.30) creates external forces

$$\begin{aligned} \mathbf{F}_{O,ap}(\mathbf{r},\ t) &= 2iq\Phi_0 \mathbf{k} \exp[i(\mathbf{k}\cdot\mathbf{r} + \omega t)], \\ \mathbf{F}_{H,ap}(\mathbf{r},\ t) &= -iq\Phi_0 \mathbf{k} \exp[i(\mathbf{k}\cdot\mathbf{r} + \omega t)], \end{aligned} \tag{3.31}$$

on the oxygen and hydrogen ions, respectively. Thus, the Liouville equation for the time-dependent phase density $f^{(3N)}(\mathbf{r}_1, \ldots, \mathbf{p}_{3N},\ t)$ in the presence of the field can be written as

$$\frac{\partial}{\partial t} f^{(3N)}(\mathbf{r}_1, \ldots, \mathbf{p}_{3N},\ t) = i\mathcal{L}(t) f^{(3N)}(\mathbf{r}_1, \ldots, \mathbf{p}_{3N},\ t), \tag{3.32}$$

with Liouville operator

$$\mathcal{L}(t) = i \sum_{j=1}^{3N} \left(\frac{\mathbf{p}_j}{m_j} \cdot \nabla_{\mathbf{r}_j} + \mathbf{F}_j(t) \cdot \nabla_{\mathbf{p}_j} \right). \tag{3.33}$$

The force $\mathbf{F}_j(t)$ is the sum of interparticle and external forces, with explicit time dependence resulting entirely from the latter contribution.

The dielectric constant $\epsilon(k, \omega)$ may be defined phenomenologically by the relation

$$4\pi \mathbf{P}(\mathbf{r},\ t) = \left(1 - \frac{1}{\epsilon(k,\ \omega)}\right) \mathbf{E}_{ap}(\mathbf{r},\ t) \tag{3.34}$$

between the polarization $\mathbf{P}(\mathbf{r},\ t)$ and the applied electric field,

$$\mathbf{E}_{ap}(\mathbf{r},\ t) = -\nabla \Phi_{ap}(\mathbf{r},\ t) = -i\Phi_0 \mathbf{k} \exp[i(\mathbf{k}\cdot\mathbf{r} + \omega t)], \tag{3.35}$$

while the induced charge density is determined in usual fashion by the divergence of the polarization,

$$\begin{aligned} \rho_{ind}(\mathbf{r},\ t) &= -\nabla \cdot \mathbf{P}(\mathbf{r},\ t) \\ &= -\frac{\Phi_0 k^2}{4\pi} \left(1 - \frac{1}{\epsilon(k,\ \omega)}\right) \exp[i(\mathbf{k}\cdot\mathbf{r} + \omega t)]. \end{aligned} \tag{3.36}$$

By familiar techniques of linear response theory, we can evaluate the induced charge on a microscopic level, provided that the external field is small enough in magnitude. The Liouville operator is first expressed as

$$\mathcal{L}(t) = \mathcal{L}_0 + \mathcal{L}_1(t), \tag{3.37}$$

where $\mathcal{L}_0$ governs the system evolution in the absence of external forces, and $\mathcal{L}_1(t)$ includes the perturbing field. A corresponding resolution into perturbed and unperturbed contribution is made for the phase density $f^{(3N)}$, whereupon elementary algebraic manipulations yield the following relation for the perturbed density, to first order:

$$f_1^{(3N)}(\mathbf{r}_1, \ldots, \mathbf{p}_{3N}, t) = \beta \sum_{j=1}^{3N} \int_{-T}^{t} ds \exp[i\mathcal{L}_0(t-s)] f_0^{(3N)}(\gamma_1(s), \ldots, p_{3N}(s)) \frac{\mathbf{p}_j(s)}{m_j} \cdot \mathbf{F}_{j,\mathrm{ap}}(s) . \tag{3.38}$$

This equation is understood in the limit as $T \to \infty$.

Since the dielectric constant at wavevector k is most naturally related to the corresponding Fourier component of the charge density, we define

$$\sigma(\mathbf{k}) = \frac{1}{\sqrt{N}} \sum_{j=1}^{3N} q_j \exp[i\mathbf{k} \cdot \mathbf{r}_j] . \tag{3.39}$$

It follows that the ensemble average of $\dot{\sigma}(\mathbf{k}', t)$ at time t is

$$\langle \dot{\sigma}(\mathbf{k}', t) \rangle = \int d\{\mathbf{r}\} \int d\{\mathbf{p}\} \dot{\sigma}(\mathbf{k}', t) f^{(3N)}(\mathbf{r}_1, \ldots, \mathbf{p}_{3N}, t)$$

$$= -\beta \Phi_0 \sqrt{N} \exp(i\omega t) \int_{-\infty}^{t} ds \exp[-i\omega(t-s)] \times \langle \dot{\sigma}(\mathbf{k}', t) \dot{\sigma}(\mathbf{k}, s) \rangle_{\mathrm{eq}} . \tag{3.40}$$

In contrast to the initial computation, the final average under the integral sign is evaluated over an equilibrium ensemble. After a change of integration variables, (3.40) yields

$$\langle \dot{\sigma}(\mathbf{k}', t) \rangle = -\beta \Phi_0 \sqrt{N} \exp(i\omega t) \times \int_{-\infty}^{0} ds \exp(i\omega s) \langle \dot{\sigma}(\mathbf{k}', -s) \dot{\sigma}(\mathbf{k}, 0) \rangle_{\mathrm{eq}} \tag{3.41}$$

for the Fourier transform of the current density.

At this point we must introduce a connection between the microscopic and phenomenological pictures in order to derive a microscopic representation of the dielectric function. Since the averaged quantities $\langle \sigma(\mathbf{k}', t) \rangle$ deviate from zero solely because of the external field, we equate these averages with spatial Fourier transforms of the macroscopic induced charge density,

$$\langle \sigma(\mathbf{k}', t) \rangle = \frac{1}{\sqrt{N}} \int_V d\mathbf{r}\, \rho_{\mathrm{ind}}(\mathbf{r}, t) \exp(i\mathbf{k}' \cdot \mathbf{r}) , \tag{3.42}$$

where the integral spans the system volume V.

Equations (3.36), (3.41), and (3.42) may be combined to give the desired formula for $\epsilon(\mathbf{k}, \omega)$. It is found that

$$1 - \frac{1}{\epsilon(k, \omega)} = \frac{-4\pi i \beta N}{\omega k^2 V} \int_{-\infty}^{0} ds \exp(i\omega s) \langle \dot{\sigma}(-\mathbf{k}, -s) \dot{\sigma}(\mathbf{k}, 0) \rangle_{\mathrm{eq}} . \tag{3.43}$$

With the aid of Eq. (3.43) we can effect the traditional separation of the conductive and dielectric screening responses of the system of ions. To obtain the dc conductivity, we combine a local version of Ohm's law, $\mathbf{J}(\mathbf{r}, \omega) = \sigma(\omega)\mathbf{E}(\mathbf{r}, \omega)$, with the macroscopic equation of continuity,

$$\dot{\rho}_{\mathrm{ind}}(\mathbf{r}, t) = -\nabla \cdot \mathbf{J}(\mathbf{r}, t) , \tag{3.44}$$

in the limit of a perturbing field of long wavelength ($k \to 0$). In view of the relation between the total and applied fields, we discover that

$$\sigma(\omega) = (i\omega/4\pi) \lim_{k \to 0} [\epsilon(k, \omega) - 1] . \tag{3.45}$$

At zero frequency the conduction current will be in phase with the perturbation, so the imaginary part of $\sigma(\omega)$ should vanish. One therefore concludes that[25]

$$\frac{1}{\sigma(0)} = \frac{N\beta}{V} \lim_{\omega \to 0} \lim_{k \to 0} \left(\frac{4\pi}{\omega k}\right)^2 \int_{-\infty}^{0} ds \cos(\omega s) \langle \dot{\sigma}(-\mathbf{k}, -s) \dot{\sigma}(\mathbf{k}, 0) \rangle_{\mathrm{eq}} . \tag{3.46}$$

Through similar reasoning, one derives an expression for the dielectric screening in the limit of zero frequency:

$$\frac{1}{\epsilon(\mathbf{k}, 0)} = 1 - \frac{4\pi\beta\rho}{k^2} \langle \sigma(-\mathbf{k}, 0) \sigma(\mathbf{k}, 0) \rangle_{\mathrm{eq}} . \tag{3.47}$$

Because water is a conducting fluid, it will be able to completely shield fields of very long wavelength. It must therefore be true that

$$\lim_{k \to 0} [1/\epsilon(\mathbf{k}, 0)] = 0 , \tag{3.48}$$

and insertion of the electroneutrality and second-moment conditions into (3.47) assures us that this is so. Because of inherent physical limitations, the short wavelength limit of $1/\epsilon(\mathbf{k}, 0)$ must be unity. In between the two extremes, for $|\mathbf{k}|$ greater than the inverse of Debye's screening length, $\epsilon(\mathbf{k}, 0)$ will take on the value commonly associated with water, ≈ 80 at room temperature.

IV. DIMER CONFIGURATIONS

As explained in Sec. II, the set of central potentials (2.6)–(2.8) has been determined by a fit of simple functional forms to important structural and energetic properties of the isolated H_2O monomer, and, in addition, to a dimer hydrogen bond energy which matches the ST2 value for a symmetric eclipsed (SE) configuration [see Fig. 2(a)]. We believe that a similar triad of central potentials can be found which will reproduce the physical properties of water at high density in computer simulation, and will also be amenable to more direct theoretical treatment, such as the integral equation[26] or mode expansion[27] techniques which have been widely exploited in recent years for simple fluids.

It is our eventual goal to subject the central-force model of water to a thorough analysis under condensed phase conditions, in an attempt to determine the exact parameter values which will lead to a realistic model fluid. However, the novelty of the central-force approximation for a polyatomic fluid as complex as water suggests a less direct initial approach. Accordingly, we have performed first a set of configurational studies of small polymers and solvated ions of water. The purpose here was to thoroughly explore the multidimensional potential surfaces characterizing two- or three-molecule interactions. This section reports the results of these configurational studies for the water dimer.

At the very least, we believe, such a characterization of the potential surfaces should be useful in uncovering stable polymers of unreasonable structure. We emphasize, in this regard, the unusual nonmonotonic behavior of the hydrogen–hydrogen interaction (2.7). The well-developed local minimum in v_{HH} could conceivably give

rise to globally stable bifurcated dimers or metastable "trapped" arrangements in the liquid. As important as the question of mechanical stability, however, is the possibility of correlating small polymer potential surfaces with the pair distribution functions evaluated in simulation runs, a process which should enable us to overcome the macroscopic deficiencies of the initial set of potentials suggested here. Through iterative fine tuning in this manner, an accurate set of effective pair potentials for water should finally emerge.

We begin the present dimer studies by looking for the minimum-energy configuration corresponding to the set of potentials (2.6)–(2.8). In order for the fitting operation described above to be regarded as valid, the best dimer structure of this configuration space search should be close to the ST2–SE arrangement. That this has, in fact, been found lends qualitative support both to the details of the fitting procedure and the central-force model in general. The investigation of dimer structures was carried out by means of a multidimensional pattern-searching subroutine.[28] Application of a variational principle to the problem of energy minimization is possible, of course, but fully unconstrained dimers possess many degrees of freedom, so this option is probably less attractive from a computational standpoint.

The nature of the pattern-searching algorithm which we employed determined the most efficient course of computation: Starting from a reasonable guess at the minimum-energy structure with relatively few degrees of freedom, the optimal dimer is evaluated in a highly restricted subspace of the full configuration space of the six independent ions. The constraints are then relaxed in a stepwise manner, with the final, lowest-energy structure of each calculation providing a new set of initial conditions for a dimer in a somewhat enlarged subspace. Throughout the computations, we impose a symmetry constraint which requires the C_2 axis of the acceptor molecule to lie in the molecular plane of the donor. By relaxing the internal molecular constraints in an intelligent manner, this procedure not only generates a sequence of restricted minimum-energy dimers, but also elucidates the energetic contributions of different types of intramolecular deformations to the dimer. As stressed in the Introduction, an analysis of such static distortions, and of the time-averaged (possibly anharmonic) vibrations that occur in dimers and larger water polymers should be important in refining the statistical mechanical theory of water.

Results of the dimer calculations are summarized in Table I; the relevant angles and distances are defined as in Fig. 2. As a point of reference, the energy of two noninteracting, undistorted molecules is given, as is the energy of two undistorted molecules in the ST2–SE arrangement. Upon searching the entire undistorted-molecule pair configuration space, the energy is lowered by about 0.1 kcal/mole when the molecules separate to an OO distance of 2.870 Å, the acceptor flaps downward to an angle of 63.1°, and the donor molecule rotates upward very slightly.

We now remove the constraints that limit each molecule to the equilibrium geometry of an isolated H_2O monomer. Allowing internal bond angles to relax first, we find a small increase in stabilization, ≈ 0.02 kcal/mole, accompanied by small changes in the other parameters of interest. Both intramolecular angles decrease somwhat. Finally, relaxing the OH bond-length constraint, the dimer of absolute minimum energy [shown in Fig. 2(b)] is determined in the full eight-dimensional symmetry-restricted configuration space. The resulting structure is characterized by a hydrogen bond energy of 6.691 kcal/mole; variation of the bond lengths has stabilized the dimer by almost 0.1 kcal/mole. As anticipated, the optimal dimer geometry is only slightly perturbed from the ST2–SE structure.

It is instructive to consider the nature of the differences between the stable dimer structure of the central-force model and the undistorted ST2–SE dimer. The hydrogen bond shown in Fig. 2(b) displays a small departure from linearity, $\approx 1°$, comparable to the ST2–SE form, and occurs at the somewhat larger OO distance of 2.865 Å. From Table I we observe that the acceptor molecule is flapped down at a larger angle, $\approx 61°$%, an effect that undoubtedly results from the increased hydrogen bond length.

On an intramolecular level, the distortions from equilibrium geometry are in qualitative agreement with

TABLE I. Parameters characterizing minimum-energy dimers of the central force model, subject to various constraints. Angles and distances defined in Fig. 2. Computations performed by pattern searching.

Dimer system	E_{MIN} (kcal/mole)	R_{12} (Å)	α (deg)	θ (deg)	θ_1 (deg)	θ_2 (deg)	Bond Lengths (Å)
Noninteracting, undistorted molecules	−225.8103	...	...	...	104.45	104.45	0.9584
Undistorted molecules, ST2–SE hydrogen bond	−232.3103	2.852	1.335	51.8	104.45	104.45	0.9584
Undistorted molecules	−232.3971	2.870	1.56	63.1	104.45	104.45	0.9584
Bond-length constrained molecules	−232.4167	2.869	1.37	62.9	103.30	104.06	0.9584
Unconstrained molecules	−232.5012	2.865	0.96	60.7	102.18	105.01	0.9602, 0.9714[a] 0.9602, 0.9602

[a]OH bond length along the hydrogen bond.

what is expected on the basis of a simple picture of the hydrogen bond as a bond between a weak Brönsted acid (the donor) and a weak Brönsted base (the acceptor). The unconstrained values of θ_1, θ_2, and the bond lengths also support the view that nonadditivity should contribute to the formation of sequences of hydrogen bonds in liquid water. By means of these geometry changes molecule 1, the donor, becomes a better acceptor for subsequent hydrogen bonds, and molecule 2, a better donor. Finally, we note that monomer distortion enhances the dipole moment of the dimer about 9% above the vector sum for two rigid molecules. These findings are in accord with a number of Hartree–Fock SCF–MO calculations.[29,30]

To provide some additional justification for the central potentials, let us compare at this point the minimum-energy dimer of Fig. 2(b) with the most favorable structures that have been calculated quantum mechanically and with those that are entailed by other phenomenological potentials that have been suggested. The large basis set calculations of Popkie, Kistenmacher, and Clementi (referred to as PKC),[31] presumably near the Hartree–Fock limit, predict a linear hydrogen bond of length 3.00 Å and magnitude 4.60 kcal/mole, with acceptor molecule hydrogens pendant at an angle of 30°. These HF computations neglect correlated fluctuations of the electron distributions in each molecule. Such correlated electronic motion, which gives rise to London dispersion interactions, can be included in the quantum pair potential in a simple empirical fashion[32] based on a scaling argument of Slater and Kirkwood[33] for the polarizability of closed-shell atomic systems. When the coefficient of the inverse sixth power attractive dispersion forces is incorporated in the PKC functional fit to the HF pair potential, the dimer of minimum energy exhibits a compression of the linear hydrogen bond to 2.855 Å, with stabilization energy raised to 6.123 kcal/mole. These values compare favorably with corresponding parameters in the central-force model.

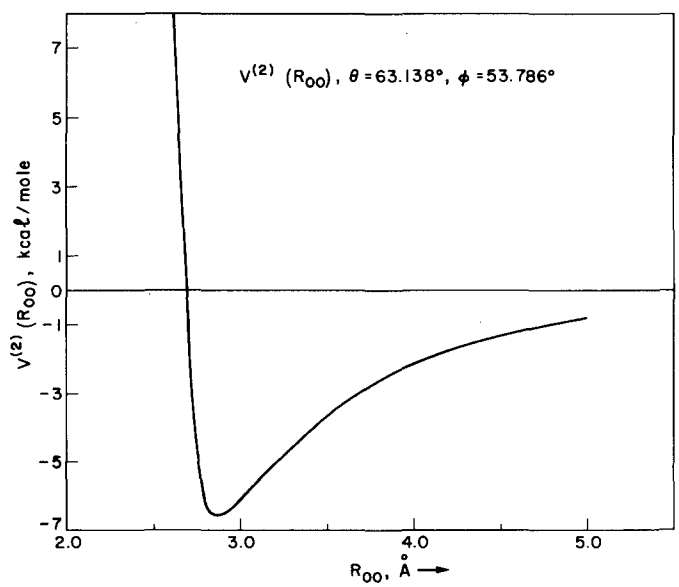

FIG. 4. Central-force model energy of interaction between two (rigid) water molecules $V^{(2)}$, as a function of oxygen–oxygen separation R_{OO}. Acceptor and donor angles defined in Fig. 2(a).

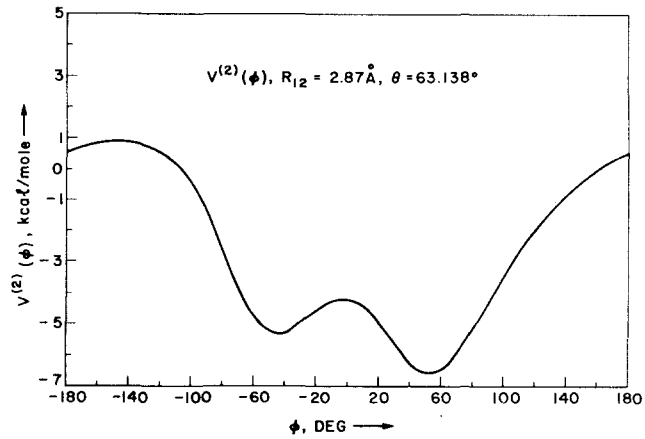

FIG. 5. Central-force model energy of interaction between two (rigid) water molecules, $V^{(2)}$, as a function of donor angle φ.

As a rule, the phenomenological models which have been used to study water molecule interactions produce somewhat shorter hydrogen bonds and larger stabilization energies than the quantum mechanical calculations indicate. This is true of the minimum-energy dimer resulting from the ST2 potential (which was described in Sec. II), and also holds for the BNS and Rowlinson interactions. The most stable BNS dimer has R_{OO} = 2.76 Å, θ = 54.7°, φ = 54.7°, with stabilization energy of 6.887 kcal/mole. For the older Rowlinson model, we have corresponding values R_{OO} = 2.69 Å, θ = 51.0°, φ = 51.9°, and 5.404 kcal/mole stabilization.

In addition to the pair configurations of minimum energy—those which exhibit mechanical stability—it is also relevant to examine the energy variation near the minimum as a function of the intermolecular coordinates. Recognizing that the *qualitative* features of the energy variation are of primary interest, we can explore this topic most productively by evaluating $V^{(2)}$ (R_{12}, θ, φ), the molecular "pair potential," for two molecules frozen in the stable monomer geometry. With angles fixed at θ = 63.1°, φ = 53.8°, the dependence of $V^{(2)}$ on OO separation is depicted in Fig. 4. The minimum at 2.870 Å is bracketted by sharply repulsive interactions at short range and an attractive tail for $R_{12} > 2.870$ Å which, as expected, is asymptotic to the dipole–dipole potential for two monomers at fixed relative orientation. The potential rises through zero at a distance of R_{12} = 2.70 Å.

Figure 5 exhibits the dependence of $V^{(2)}$ on φ, the donor angle, assuming the optimal values for R_{12} and θ given in Table I. The curve displays asymmetric local minima, with an intervening local maximum at $\varphi = 0°$, when the oxygen of the acceptor molecule is equidistant from both hydrogens of the donor. The barrier to donor rotation, if measured from the higher of the two minima, is $\approx$ 1.1 kcal/mole; the degree of asymmetry of the wells, which reflects the differing interactions of nonbonded hydrogens, is 1.2 kcal/mole.

The behavior of the energy variation curves for the

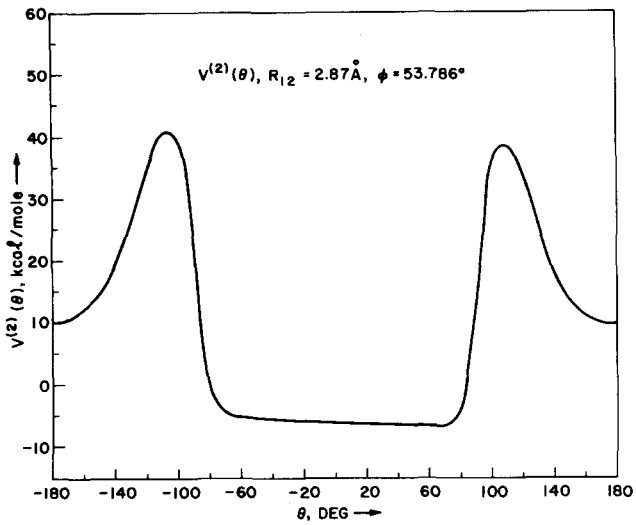

FIG. 6. Central-force model energy of interaction between two (rigid) water molecules, $V^{(2)}$, as a function of acceptor angle θ. Prominent peaks near $\pm 110°$ are discussed in the text.

central-force model is thus far quite similar, qualitatively, to that manifested by the other phenomenological models we have mentioned. We note a number of differences, however, upon examining the functional dependence of $V^{(2)}$ on θ, shown in Fig. 6. The appearance of two rather prominent maxima centered at $\pm 110°$ would seem, at first glance, to be an unrealistic feature of the intermolecular interactions. These peaks, and the sharp declines in $V^{(2)}$ for $|\theta| > 110°$, represent the effect of nonmonotonicity in the hydrogen–hydrogen interactions. With R_{12} and φ fixed at the indicated values, the protons on the two molecules approach each other most closely when $\theta \approx 175°$, where the curve $V^{(2)}(\theta)$ has a local minimum.

It is not difficult to see that, at ordinary temperatures, the unusual behavior of $V^{(2)}(\theta)$ near $\pm 180°$ should have little effect on the equilibrium configurations or thermally activated vibrations of small polymers of H_2O, because the local minimum occurs some 15 kcal/mole higher than the absolute minimum at $\theta = 61°$. By similar reasoning one deduces that this anomaly in the potential $V^{(2)}(\theta)$ will have negligible effect on an ensemble of H_2O molecules at liquid densities, not only because of the thermally unfavorable Boltzmann factor, but also because effective hard core repulsions in the liquid should screen out this region of $V^{(2)}(\theta)$. We therefore regard the local minimum in $V^{(2)}(\theta)$ as physically irrelevant for either small clusters or condensed phases—a supposition which has been validated, *a posteriori*, by explicit calculations.

Let us proceed now to examine the energy variation in the central region bounded by $|\theta| \lesssim 70°$. A comparison of Fig. 6 with similar graphs for the ST2 and BNS potentials reveals the absence of a double minimum in this angular range for our model. In the ST2 and BNS potentials such structure in $V^{(2)}(\theta)$ exists as a consequence of the explicit inclusion of tetrahedral coordination in the monomer geometry by means of negative charges emerging from the back of each molecule. These charges are supposed to represent nearly sp^3-hybrid lone pair orbitals. But although the BNS and ST2 models offer reasonable ways to approximate the effective molecular pair potentials,[34] it should be observed that *ab initio* quantum calculations imply that the role of sp^3 hybridization has been overestimated in hydrogen bond formation in water.[29] In the calculations of Popkie, Kistenmacher, and Clementi, for example, the dimer energy in a restricted acceptor angle subspace manifests no central double minimum. In fact, in the range of angles θ which are probably important for liquid water, from $\theta = -60°$ to $\theta = +60°$, the PKC energy varies by 1.1 kcal/mole, which compares favorably with the corresponding value, 1.3 kcal/mole, for the present model.

The set of dimer calculations summarized in the present section appears to be a promising sign for the representability of water molecule pair interactions by a set of central potentials acting between atomic species. Both the optimum dimer structure and the nature of the energy variation near the minimum seem to be reproduced relatively well by the set of simple functions (2.6)–(2.8). While the energy variation departs for some orientations from the behavior of other model potentials, the departures resemble quantum mechanical results. In any case, such configurations should not be important for the real liquid.

V. TRIMER CONFIGURATIONS

In order to characterize more fully the structural implications of the triad of central potentials, the pattern search was utilized to determine the most favorable configuration of the water trimer, $(H_2O)_3$. As for the dimer, the most productive strategy was to start with a small number of educated guesses for the trimer structure of lowest energy, and to perform searches in a sequential manner in configuration subspaces of increasing dimensionality. In order to extract physically meaningful observations from these searches without inordinate computational effort, each molecule was assumed in the equilibrium geometry initially, and subsequently the bond angles were allowed to vary.

The general configurations employed as initial guesses in the minimization were the canonical arrangements that are usually termed the double donor, double acceptor, and serial trimers (see Fig. 7). The first two, as the nomenclature implies, include central molecules which either donate or accept two protons, respectively. In the serial trimer, by contrast, the central H_2O is a donor in one hydrogen bond and an acceptor molecule in a second. The starting configurations selected were generally symmetrical, and the energy minimization was initially attempted with all three molecules restricted to a single plane.

The outcome of these planar searches is illustrated in Fig. 8; the geometric and energetic parameters characterizing the trimers are summarized in the upper portion of Table II. The lack of congruence among the three resulting structures indicates a planar trimer potential surface which is extremely flat in certain re-

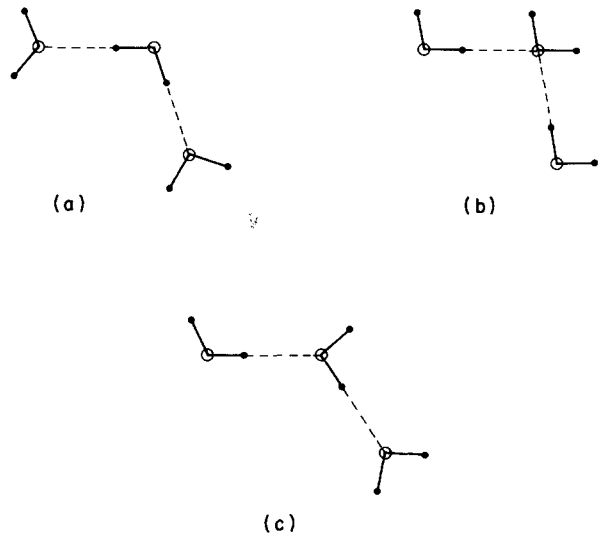

FIG. 7. Schematic planar projection of the three fundamental water trimers: (a) double donor, (b) double acceptor, (c) serial.

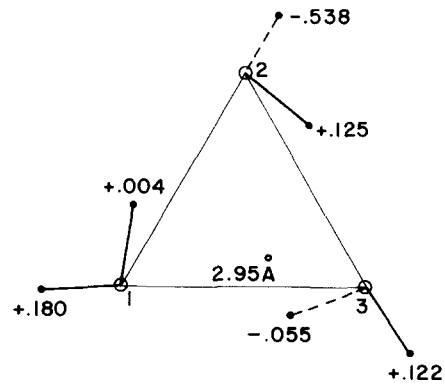

E_{STAB} = 18.062 kcal/mole

θ_1 = 103.11°, θ_2 = 103.16°, θ_3 = 103.16°

FIG. 9. Optimum nonplanar trimer found. As an indication of distance scale, one of the OO separations is shown. The extent to which each hydrogen lies outside of the OOO plane is also given quantitatively, in Å. Legend specifies the three internal bond angles and stabilization energy.

gions, where the pattern search becomes relatively inefficient. It also implies that the pattern search, like other minimization algorithms, is prone to becoming "trapped" near regions of local minima. We attempted to overcome the latter difficulty by conducting several searches near the apparent "minimum" with widely differing initial step sizes. Most of the time this approach was successful in dealing with local wells on the potential surface. We are confident that the single lowest-energy structure which has been found by this procedure does correspond to the global minimum (in the appropriate restricted subspace), since that minimum has been approached from several low-energy directions.

In a manner similar to that described in Sec. IV, the constraint requiring all hydrogens to lie in the plane of the three oxygen ions was relaxed, and the pattern search was next applied to an investigation of nonplanar three-molecule structures. The final planar configurations were used as points of departure. Quantitative detail resulting from these searches is contained in the lower section of Table II. All calculations gave rise to a minimum-energy trimer with three oxygen ions arranged in a nearly equilateral triangle. This array possesses three highly strained hydrogen bonds, with hydrogen ions situated above and below the OOO plane in such a way as to minimize the unfavorable HH interactions. Of course, since the cyclic trimer forms an odd-numbered polygon, the H's on neighboring molecules cannot be entirely staggered.

It is interesting to note that all of the planar initial configurations lead to the compact, nearly equilateral trimer, and it is this consistent result which encourages us to believe that the lowest-energy nonplanar form (see Fig. 9), which is produced by the serial starting configuration, is in fact very near the global minimum on the relevant trimer potential surface. This idea was confirmed by a direct calculation which started from a triangular trimer with pronounced nonplanar geometry.

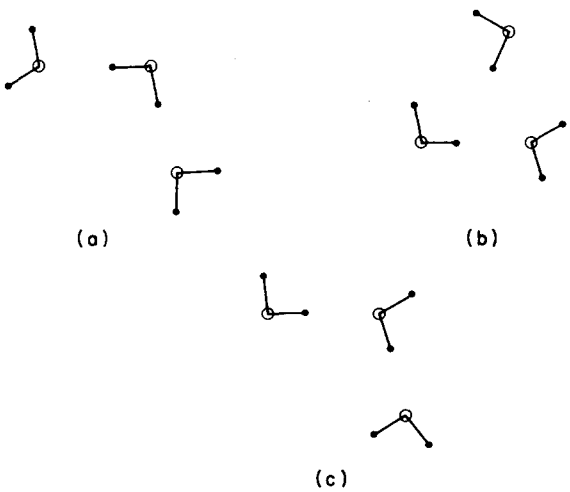

FIG. 8. Outcome of planar trimer pattern searches, starting from (a) double donor, (b) double acceptor, (c) serial configurations. The serial planar arrangement is energetically most favorable.

TABLE II. Geometric and energetic parameters for planar and nonplanar configurations.

Initial Configuration	Stabilization Energy[a] (kcal/mole)	Internal Bond Angles θ_1, θ_2, θ_3 (deg)
Planar		
Double Donor	12.060	104.18, 102.31, 104.20
Double Acceptor	11.866	104.30, 103.36, 105.44
Serial	13.868	102.73, 102.89, 103.56
Nonplanar		
Double Donor	16.493	103.68, 102.12, 103.73
Double Acceptor	16.710	102.23, 103.76, 103.34
Serial	18.062	103.11, 103.16, 103.16

[a]Stabilization with respect to three noninteracting H_2O molecules.

The trimer calculations on central-force water are a reassuring indication that the hydrogen bond built into potentials (2.6)–(2.8) for the water dimer produces no unreasonable results for the trimer. The most stable structure of these particular interactions resembles the cyclic trimer found most favorable in small basis set quantum mechanical computations,[35] although the OO distances are here somewhat larger (≈2.95 Å) and more representative of real water. While more extensive Hartree–Fock calculations[29] suggest that the serial configuration is competitive because of decreased ring strain, the relatively compact cyclic arrangement might be intuitively expected for a classical point-charge model.

(*Note added in proof*: Kistenmacker *et al.* [J. Chem. Phys. 61, 546 (1974)] have recently evaluated minimum energy structures for small clusters of water molecules, employing an analytic fit to the Hartree-Fock intermolecular potential.[31] For the trimer, the resulting structure is in good agreement with Fig. 9.)

VI. HYDRONIUM ION

With the aid of potentials v_{OH}, v_{HH}, and v_{OO} one may evaluate a number of structural and energetic features of hydrated protons or hydroxyl ions. Such species are extremely important in charge-transfer processes in pure H_2O, and also play a role in determining the chemical and physical properties of various hydrated salts. Here we treat the singly hydrated proton H_3O^+. (In writing out this species we neglect the fact that the excess proton bears only a partial charge.)

The mechanically stable hydronium ion is pyramidal, with three equivalent OH bonds of length r_{OH}, the monomer bond length. The axial angle between each OH bond and the pyramid altitude is 66°. These parameters are only slightly smaller than values reported for real H_3O^+.[36] Figure 10 displays the dependence of H_3O^+ binding energy on the axial angle φ_0, assuming the OH distance is optimized for each φ_0. The double-welled curve which results effectively gives the energy barrier to H_3O^+ inversion, 4.9 kcal/mole. This value compares reasonably well with values computed by self-consistent field methods.[37]

VII. DISCUSSION

We have outlined above a number of properties which should be amenable to calculation with a central-force model of water, once the pair correlation functions of the liquid have been evaluated. While molecular dynamics is always available as one means of computing them, it is our eventual goal to apply integral equation methods to this problem. Extensions of the convoluted hypernetted-chain equations (CHNC) seem promising on this front, as these techniques have been recently applied to the study of electrolytes in aqueous solution with some success.[38] At the present level of theoretical development, it is probably impossible to solve these equations for liquids with strongly noncentral interactions.

Preliminary tests of the specific set of potentials (2.6)–(2.8) in short-duration molecular dynamics runs indicate that these interactions are not entirely satisfactory. Examination of the OO pair correlation function from such a run reveals the difficulty with these particular functions: the oxygen cores exhibit too great a tendency towards close packing. It appears that the hydrogen bonds implied by these potentials are prevented from producing an open tetrahedral network by strong indirect contributions to the intermolecular potential of mean force, and as a result the liquid collapses partially toward a system of close-packed molecules. Minor modifications of (2.6)–(2.8) seem to correct this deficiency, however, leading to the nearly tetrahedral order that is characteristic of water. Molecular dynamics

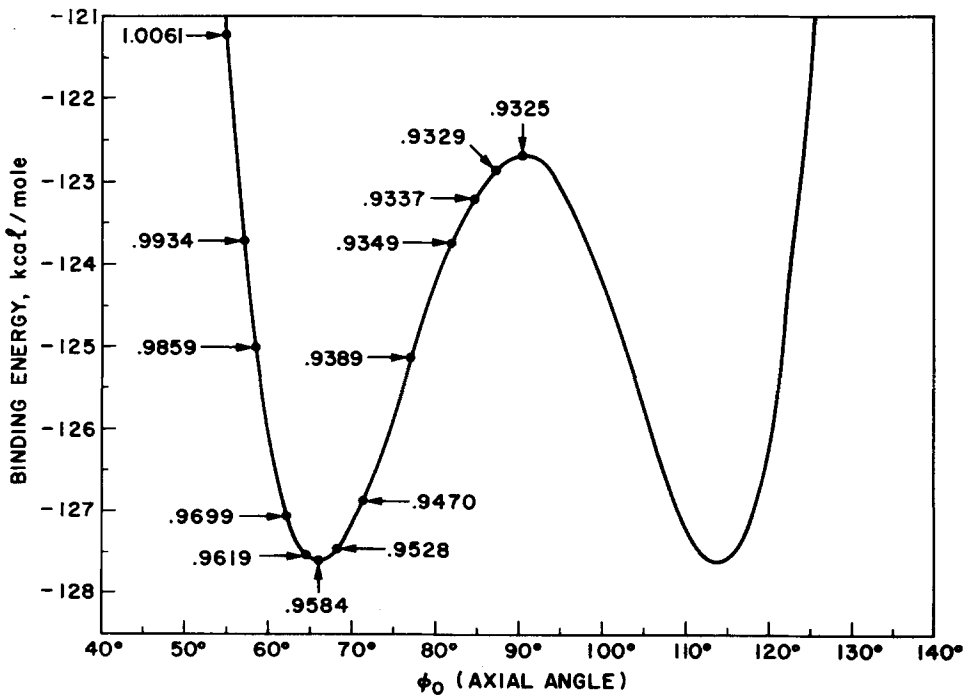

FIG. 10. Hydronium ion inversion barrier: dependence of H_3O^+ binding energy on axial angle φ_0.

for this improved set of potentials, as well as numerical solution of the HNC equations, will be reported at a later date.

The simplicity and computational efficiency promoted by a central-force model of water should make possible several theoretical investigations in addition to those suggested in Sec. III. A significant number of nonequilibrium properties previously inaccessible to molecular models might be evaluated: infrared and Raman bandshapes for intramolecular modes, the kinetics of proton-transfer reactions, and the rate and extent of self-dissociation of water at high temperatures and pressures[39] are among those of great interest. From the point of view of solution chemistry, simple elaborations of the present model should facilitate the study of solute–solvent interactions on a truly microscopic scale. It would be particularly interesting to examine the alteration of solvent structure and transport properties in the tightly bound solvation shell centered on spherically symmetric ions in strong electrolytes. The study of "bound water" interactions is also of great importance for nonpolar solutes, as the hydrophobic effect is essential in modulating the characteristics of lipid bilayer membranes.[40]

While the present paper has limited attention to liquid water, there is in principle no barrier to applying a central-force model to other polyatomic fluids. Since internal molecular degrees of freedom must be incorporated in a highly restricted configuration subspace, "simple" polyatomic liquids are undoubtedly best suited to such a treatment. Two other hydrogen bonded substances, HF and NH_3, would seem good candidates for central-force models.

ACKNOWLEDGMENT

We wish to thank Dr. Aneesur Rahman for aid in performing molecular dynamics simulations on central-force water, and for stimulating discussions during the execution of this work.

[1]A recent overview of the theory and molecular models of water is provided by F. H. Stillinger, Adv. Chem. Phys. (to be published).
[2]B. J. Alder and T. Wainwright, in *Transport Processes in Statistical Mechanics*, edited by I. Prigogine (Interscience, New York, 1958), p. 97.
[3]N. Metropolis, A. W. Rosenbluth, N. M. Rosenbluth, A. H. Teller, and E. Teller, J. Chem. Phys. 21, 1087 (1953).
[4]A. Rahman and F. H. Stillinger, J. Chem. Phys. 55, 3336 (1971); F. H. Stillinger and A. Rahman, *ibid.* 57, 1281 (1972).
[5]A. Rahman and F. H. Stillinger, Phys. Rev. A 10, 368 (1974); F. H. Stillinger and A. Rahman, J. Chem. Phys. (to be published).
[6]A. Ben-Naim and F. H. Stillinger, in *Water and Aqueous Solutions*, edited by R. A. Horne (Wiley-Interscience, New York, 1972), Chap. 8.
[7]F. H. Stillinger and A. Rahman, J. Chem. Phys. 60, 1545 (1974).
[8]P. D. Fleming III and J. H. Gibbs, J. Stat. Phys. 10, 157 (1974).
[9]G. M. Bell, J. Phys. C 5, 889 (1972).
[10]O. Weres and S. A. Rice, J. Am. Chem. Soc. 94, 8984 (1972).
[11]A. Ben-Naim, J. Chem. Phys. 54, 3682 (1971).
[12]J. D. Bernal and R. H. Fowler, J. Chem. Phys. 1, 515 (1933).
[13]E. J. W. Verwey, Recl. Trav. Chim. Pays-Bas 60, 887 (1941).
[14]J. S. Rowlinson, Trans. Faraday Soc. 47, 120 (1951).
[15]N. Bjerrum, Science 115, 385 (1952).
[16]L. L. Shipman and H. A. Scheraga, J. Phys. Chem. 78, 909 (1974).
[17]T. R. Dyke and J. S. Muenter, J. Chem. Phys. 59, 3125 (1973).
[18]C. W. Kern and M. Karplus, in *Water, A Comprehensive Treatise*, edited by F. Franks (Plenum, New York, 1972), Vol. 1, p. 37.
[19]D. Eisenberg and W. Kauzmann, *The Structure and Properties of Water* (Oxford University, New York, 1969), p. 7.
[20]Actually, the curvatures have been determined from the fundamental frequencies of D_2O, as quantum effects are smaller for vibrations of the heavier deuterium atoms. See Ref. 19.
[21]F. H. Stillinger and R. Lovett, J. Chem. Phys. 48, 3858 (1968).
[22]J. O. Hirschfelder, C. F. Curtiss, and R. B. Bird, *Molecular Theory of Gases and Liquids* (Wiley, New York, 1954), Chap. 3.
[23]R. Zwanzig and R. D. Mountain, J. Chem. Phys. 43, 4464 (1965).
[24]E. Wigner, Phys. Rev. 40, 749 (1932); J. G. Kirkwood, *ibid.* 44, 31 (1933); 45 116 (1934).
[25]Limits must be taken in the order indicated. This point and other complications that arise in passing to the hydrodynamic limit for systems with long-range forces are treated by P. C. Martin, *Measurements and Correlation Functions* (Gordon and Breach, New York, 1968), pp. 63 ff.
[26]See, e.g., H. L. Frisch and J. Lebowitz, *The Equilibrium Theory of Classical Fluids* (Benjamin, New York, 1965).
[27]H. C. Andersen and D. Chandler, J. Chem. Phys. 53, 547 (1970).
[28]The pattern search employed here was a modification of the routine developed by O. G. Ludwig, Ph. D. thesis (Carnegie Institute of Technology, 1961). We thank Dr. T. A. Weber for pointing out this useful minimization procedure.
[29]D. Hankins, J. W. Moskowitz, and F. H. Stillinger, J. Chem. Phys. 53, 4544 (1970).
[30]K. Morokuma and L. Pedersen, J. Chem. Phys. 48, 3275 (1968); K. Morokuma and J. R. Winick, *ibid.* 52, 1301 (1970).
[31]H. Popkie, H. Kistenmacher, and E. Clementi, J. Chem. Phys. 59, 1325 (1973).
[32]For a more thorough presentation of the reasoning involved, see the discussion of this empirical correction in Ref. 1.
[33]J. C. Slater and J. G. Kirkwood, Phys. Rev. 37, 682 (1931).
[34]F. H. Stillinger, J. Phys. Chem. 74, 3677 (1970); J. Chem. Phys. 57, 1780 (1973).
[35]J. Del Bene and J. A. Pople, J. Chem. Phys. 52, 4858 (1970).
[36]P. A. Kollman and C. F. Bender, Chem. Phys. Lett. 21, 271 (1973).
[37]H. Lischka and V. Dyczmons, Chem. Phys. Lett. 23, 167 (1973).
[38]J. C. Rasaiah and H. L. Friedman, J. Chem. Phys. 48, 2742 (1968); 50, 3965 (1969).
[39]W. B. Holzapfel, J. Chem. Phys. 50, 4424 (1969).
[40]C. Tanford, *The Hydrophobic Effect* (Wiley, New York, 1973).